Synthesis, Magnetic Properties and Molecular Structure of $CuLCl_2$, where L = 2-Aminomethylpyridine (amp) and 2,2′-Aminoethylpyridine (aep). One-dimensional Antiferromagnetic Interactions in $Cu(amp)Cl_2$

CHARLES J. O'CONNOR*, ETIM E. EDUOK

Department of Chemistry, University of New Orleans, New Orleans, La. 70148, U.S.A.

FRANK R. FRONCZEK

Louisiana State University, Baton Rouge, La. 70806, U.S.A.

and OLIVIER KAHN

Laboratoire de Spectrochimie des Eléments de Transition, Univeristé de Paris-Sud, 91405 Orsay, France

Received March 6, 1985

Abstract

The synthesis, magnetic properties and molecular structure of two copper(II) chloride complexes of aminoalkylpyridines are discussed. The X-ray crystal structure of $Cu(amp)Cl_2$ (amp = 2-aminomethylpyridine) shows the compound crystallizes as a one dimensional chain with one chlorine non-bridging and the other chlorine triply bridging. The magnetic data are successfully analyzed with the Bonner-Fisher one dimensional magnetic chain model with the resulting parameters: $g = 2.06$, $J/k = 7.11$ K, $zJ'/k = -0.69$ K. The analogous complex $Cu(aep)Cl_2$ (aep = 2-2′-aminoethylpyridine) is reinvestigated using the dimer equation corrected with the molecular field approximation. The resulting parameters are $g = 2.05$, $J/k = -3.83$ K, $zJ'/k = -0.12$ K. Crystal data for $CuC_6H_8N_2Cl_2$: monoclinic, $a = 7.932(2)$ Å, $b = 6.257(1)$ Å, $c = 9.435(2)$ Å, $\beta = 112.97(2)°$, $V = 431.1(3)$ Å^3, $Z = 2$, space group $P2_1/m$.

Introduction

We are currently synthesizing copper(II) complexes in order to increase the number of model systems that may be used to elucidate structural correlations with observed magnetic interactions in those complexes that exhibit short range order. In fact, the study of magneto-structural relationships in magnetically coupled systems has become an area that several laboratories have been pursuing [1–6]. A great deal of the reported work has been concerned with binuclear copper(II) complexes, especially those bridged by hydroxide [6, 7] or chloride [8–14] ions, and several explanations have been proposed to describe the magnetic behavior of these types of exchange coupled complexes [15–24].

The bridging center geometry between four, five, and six coordinate doubly bridged metal ions is often divided into two categories. These categories are illustrated by (1) parallel plane bridging in which the bridging ligands are equatorially bound to both metal ions and (2) perpendicular plane bridging in which the bridging ligands are axially bound to one metal ion and equatorially bound to the other.

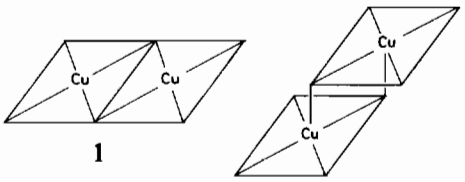

1 2

Hydroxide bridged complexes of type 1 have been empirically correlated by Hatfield and Hodgson [6, 7] and verified by several other laboratories. The situation for chlorine bridged complexes on the other hand is much more complicated, partly due to the low lying d-orbitals on the halogen that are involved in the magnetic exchange overlap pathways. Many chlorine bridged binuclear [8, 9] and polymeric [10–13] complexes have been synthesized and attempts to empirically correlate their magneto-structural properties have met with only limited success.

We have prepared complexes from copper(II) chloride and aminoalkylpyridines that crystallize into polymers of type 2. The magnetic properties and crystal structure of the complex Cu(aep)Cl has been reported previously by Hodgson *et al.* [14, 25]; however, details of the magnetic data were unclear.

*Author to whom correspondence should be addressed.

0020-1693/85/$3.30

They report a structure consisting of binuclear $[Cu(amp)Cl_2]_2$ units that are in turn bridged by chlorines to form a polymeric network. Although the authors reported that the dimer model gave a better fit to the magnetic data than the lincar chain model, no attempt was made to accommodate the interdimer (*i.e.* polymeric) interactions in their binuclear analysis. In light of our findings on the analogous $Cu(amp)Cl_2$ complex, also presented in this report, we decided to reinvestigate the magnetic properties of $Cu(aep)Cl_2$. We report here on the synthesis, molecular structure, and magnetic properties of the complexes $[Cu(amp)Cl_2]$ and $[Cu(aep)Cl_2]$ where amp = 2-aminomethylpyridine and aep = 2,2′-aminoethylpyridine.

Experimental

Syntheses

$Cu(aep)Cl_2$ was prepared by adding stoichiometric amounts of hydrated $CuCl_2$ and 2,2′-aminoethylpyridine in absolute ethanol. A blue powder consisting of fine platelike crystals then precipitated, was filtered, and dried overnight in the air. $Cu(amp)Cl_2$ was prepared in the same fashion as the $Cu(aep)Cl_2$ analog. The crystalline product was a deeper blue than $Cu(aep)Cl_2$.

Magnetic Susceptibility

Polycrystalline samples of the complexes were measured on a model 905 superconducting SQUID Susceptometer from SHE Corporation. The susceptometer is interfaced to an IBM 9000 computer system. Data were recorded over the 2.0–300 K temperature range. The general experimental technique is described elsewhere [2]. The molar magnetic susceptibility data for the two complexes, corrected for diamagnetism with Pascal's constants, are listed in Table I (Supplementary material).

X-ray

The crystal structure of Cu(2-2′-aminoethylpyridine)Cl_2 has been previously reported [14]. In our hands, these crystals yielded slightly different cell dimensions: *Pbca*, $a = 8.764(3)$, $b = 19.511(3)$, $c = 10.940(2)$ Å, $Z = 8$, $D_c = 1.823$ g cm^{-3}. These cell dimensions were determined at 25 °C by a least-squares fit of 2θ values of 25 reflections having $33° < 2\theta < 53°$, measured on an Enraf-Nonius CAD4 diffractometer with MoK_α radiation ($\lambda = 0.71073$ Å) and a graphite monochromator. Each measurement was made at $\pm 2\theta$.

Cu(2-aminomethylpyridine)Cl_2

Intensity data were collected at variable rates, designed to yield equal relative precision for all observable data (Table II). A maximum was placed on the scan time spent on any reflection. Data reduction included corrections for background, Lorentz, and polarization effects, as well as absorption corrections, based on ψ scans of reflections near $\chi = 90°$. Reflections having $I > 3\sigma(I)$ were used in the refinement.

TABLE II. Crystal Data and Data Collection Parameters.

Formula	$CuCl_2C_6H_8N_2$
Formula wt.	242.6
Space group	monoclinic, $P2_1/m$
a (A)	7.932(2)
b (A)	6.257(1)
c (A)	9.435(2)
β (deg)	112.97(2)
V (A^3)	431.1(3)
Z	2
T (°C)	23
D_c (g cm^{-3})	1.869
Radiation	MoK_α ($\lambda = 0.71073$ A)
Monochromator	graphite
μ (cm^{-1})	31.0 cm^{-1}
Diffractometer	Enraf-Nonius CAD4
Crystal size (mm)	plate, 0.12 × 0.48 × 0.52
Min. rel. transmission (%)	43.45
Scan type	-2
Scan rates (deg min^{-1})	0.42–5.0
Precision	$I \cong 50(I)$
Max-scan time (s)	180
2θ limits (deg)	2–68
h, k, l limits	0–11, 0–9, −14–14
Unique data	1887
Observed data	1343
Variables	86
R	0.035
R_w	0.051
GOF	1.600
Max-residual (eA^{-3})	0.55

Systematic absences $0k0$ with k odd require space group $P2_1$ or $P2_1/m$. A solution in the centrosymmetric group was found by heavy atom methods, and was successfully refined, requiring only a slight disorder. Refinement was by full matrix least squares based on F with weight $w = \sigma^2(F_o)$, using the Enraf-Nonius SDP programs [26], scattering factors of Cromer and Waber [27] and anomalous coefficients of Cromer [28]. Nonhydrogen atoms were refined anisotropically; hydrogen atoms were refined isotropically, except for those on the disordered atom C6, which were calculated. Final coordinates are given in Table III; anisotropic thermal parameters and structure factors are included with the supplementary material as Table IV and Table V.

Results

Analysis of the X-ray data of $Cu(amp)Cl_2$ reveals a structural linear chain. An ORTEP diagram of a

TABLE III. Coordinates and Thermal Parameters for Cu(amp)Cl_2.

Atom	*x*	*y*	*z*	*B* or B_{eq}
Cu	0.00968(4)[a]	0.25	0.09885(3)	3.376(6)
Cl1	−0.2759(1)	0.25	0.09180(9)	5.35(6)
Cl2	−0.0942(1)	0.25	−0.16196(7)	4.35(2)
N1	0.1408(3)	0.25	0.3277(2)	3.56(4)
N2	0.2628(3)	0.25	0.1043(3)	3.97(5)
C1	0.3222(4)	0.25	0.3787(3)	4.42(7)
C2	0.4331(5)	0.25	0.5335(4)	6.1(1)
C3	0.3509(7)	0.25	0.6409(4)	6.4(1)
C4	0.1654(5)	0.25	0.5893(4)	5.71(8)
C5	0.0627(4)	0.25	0.4320(3)	4.57(6)
C6[b]	0.3983(4)	0.2922(7)	0.2563(4)	4.0(1)
H2	0.535(5)	0.25	0.549(4)	4.6(9)
H3	0.414(5)	0.25	0.736(4)	4.1(8)
H4	0.086(5)	0.25	0.655(5)	5.8(10)
H5	−0.071(6)	0.25	0.383(5)	7.0(12)
H2N	0.298(4)	0.173(5)	0.057(3)	6.6(8)
H61[b]	0.501	0.202	0.275	5.0
H62[b]	0.435	0.437	0.262	5.0

[a]E.s.d.s. in the least significant digits are shown in parentheses. [b]Population = 1/2. [c]$B_{eq} = (B_{11} + B_{22} + B_{33})/3$.

chain fragment is illustrated in Fig. 1. The bridging network consists of copper(II) ions bridged by chloride ligands to form a 'ladder type' linear chain that is structurally very similar to the analogous bromine bridged complex [29]. The copper to copper separation with in the chain is 3.615(1) Å. The bridging geometry is of type **2**; the bridging chloride Cl2 is coordinated to the equatorial position of one copper (short bond, 2.270(1) Å) and the axial position of the adjacent copper (long bond 3.206(1) Å). This is, however, an oversimplification of the bridging geometry because the chloride ions are in fact triply bridging with coordination geometry consisting of two long axial Cu–Cl bonds and one short equatorial Cu–Cl bond. The rest of the copper coordination sphere is completed with the bidentate ligand (amp) bound as an equatorial chelate and a non-bridging equatorial chlorine, Cu–Cl1 2.240(1) Å. Bond distances and angles within the Cu(amp)Cl_2 molecule are given in Table IV. The square plane of the molecule lies on a crystallographic mirror plane, and is thus entirely planar except for C6, which is disordered into two equally-populated positions separated by 0.53 Å across the mirror.

An ORTEP of Cu(aep)Cl_2 is illustrated in Fig. 2. The complex crystallizes as a polymer of binuclear units. The copper(II) binuclear units with double chlorine bridges are in turn linked by single chlorine bridges to form a polymeric network. This bridging geometry results in a lattice interaction that might be expected to have properties intermediate between a dimer and a polymer. The dimer limit is attained when the interdimer coupling (J') is zero and the infinite lattice interaction will occur when the intradimer exchange (J) is equal to the interdimer exchange (J').

The magnetic susceptibility data for each of the complexes are plotted in Figs. 3 and 4. In both complexes, the magnetic data exhibit a broad maximum at low temperatures. This behavior is consistent with the presence of short range antiferro-

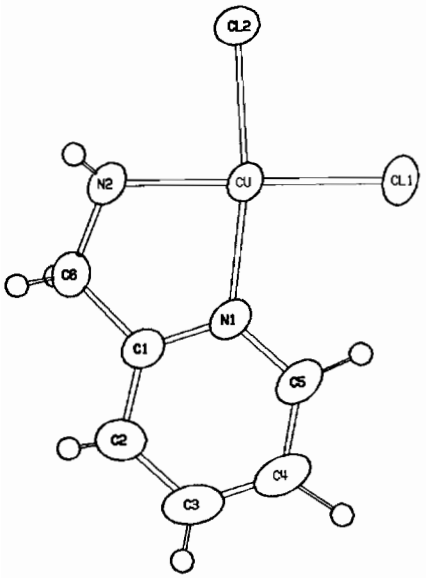

Fig. 1. ORTEP diagram of Cu(amp)Cl_2. Each structural unit is bridged to form an infinite one dimensional structural chain.

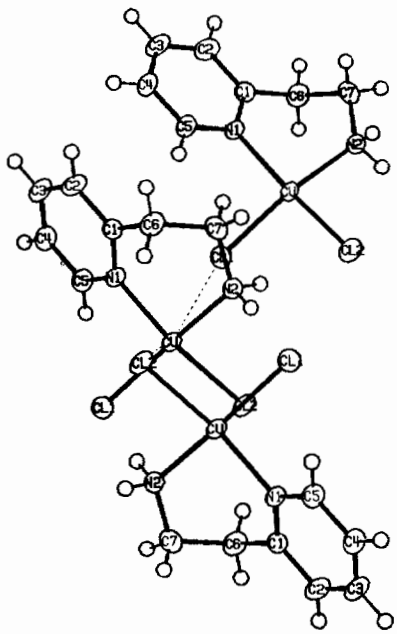

Fig. 2. ORTEP diagram of $[Cu(aep)Cl_2]_2$ binuclear unit showing interdimer chlorine bridges.

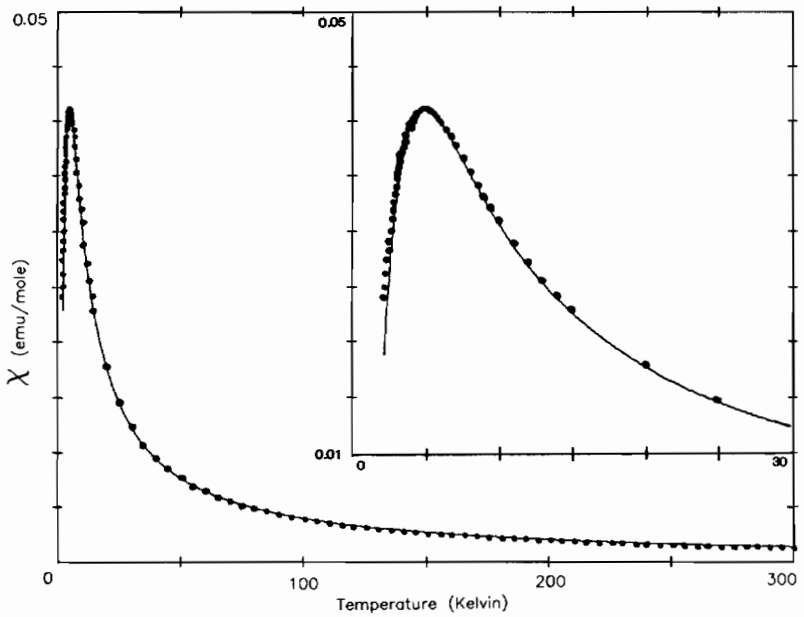

Fig. 3. Magnetic susceptibility of $Cu(aep)Cl_2$ plotted as a function of temperature. The curve through the data points is the best fit of the data to be binuclear model as described in text. The insert shows a expanded scale of the low temperature region.

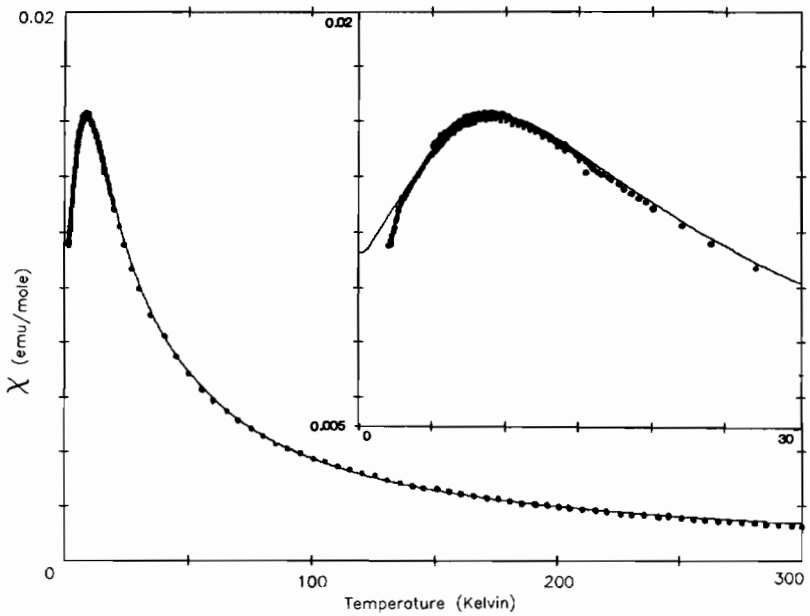

Fig. 4. Magnetic susceptibility of $Cu(amp)Cl_2$ plotted as a function of temperature. The curve through the points is the best fit of the data to the one dimensional antiferromagnetic chain model as described in text. The insert shows an expanded scale of the low temperature region.

magnetic interactions. The theoretical analysis of the magnetic data was guided by the various structural features gleaned from the X-ray studies. Fitting of the data proceeded from the simple Curie-Weiss analysis of the high temperature magnetic data to a more involved theoretical analysis of the various types of short range ordering phenomena likely to be involved in the complexes.

At elevated temperatures, the magnetic data for each complex were fitted to the Curie-Weiss law for $S = 1/2$ copper(II).

$$\chi = \frac{Ng^2\mu_B{}^2}{4k(T - \theta)} \quad (1)$$

The fitted Curie-Weiss parameters are listed in Table VII. The negative values for the Weiss constant are expected and are a result of the antiferromagnetic coupling found in the two complexes at low temperatures. As the temperature is lowered to the point where the magnetic susceptibility reaches a maximum, the data begin to deviate sharply from Curie-Weiss law. For the theoretical analysis of the data at these lower temperatures, two models were selected: the binuclear model and the linear chain model.

The primarily dimeric geometry of Cu(aep)Cl_2 indicates that the simple binuclear equation is a logical place to begin the analysis for this complex. For two interacting copper(II) ions with $S_1 = S_2 = 1/2$, the magnetic susceptibility may be described by the equation:

$$\chi = \frac{2Ng^2\mu_B{}^2}{kT} \frac{e^x}{1 + 3e^x} \quad (2)$$

where $x = 2J/kT$, and $2J$ is the energy gap between the resulting singlet and triplet states and with a negative J value denoting a singlet ground state. The data for Cu(aep)Cl_2 were fit to eqn. (2); however, a molecular field correction to the data was required before a satisfactory fit was obtained. The form of this molecular field correction is as follows [2]:

$$\chi' = \frac{\chi}{1 - (2zJ'/Ng^2\mu_B{}^2)\chi} \quad (3)$$

where χ is the uncorrected magnetic susceptibility in the absence of an exchange field (eqn. (2)), and χ' is the magnetic susceptibility actually measured. The best fit parameters from the binuclear equation (eqn. (2)) corrected for the molecular field interaction (eqn. (3)) are listed in Table VII. Figure 3 shows a plot of the fitted curve drawn through the experimental data points.

Although Cu(amp)Cl_2 is a structural linear chain, the magnetic data for this complex were analyzed with the binuclear equation to see if an acceptable fit of the data could be obtained using this simple model. The result of the fitting procedure was unsatisfactory, even when the molecular field correction was added. Moreover, the resulting parameters gave an unacceptable ratio of J'/J that is too large. As expected from the structural information, the binuclear equation clearly provides a poor model for the magnetic behavior of the Cu(amp)Cl_2.

The magnetic susceptibility data of Cu(amp)Cl_2 was then analyzed using the Bonner-Fisher linear chain model [30]. The magnetic data were fitted to the linear chain model following an interpolative

TABLE VI. Bond Distances and Angles in Cu(amp)Cl_2.

Distances (Å)	
Cu–Cl1	2.240(1)
Cu–Cl2	2.270(1)
Cu–N1	1.998(2)
Cu–N2	1.988(2)
N1–C1	1.328(4)
N1–C5	1.351(3)
Cu–Cu	3.615(1)
N2–C6	1.342(4)
C1–C2	1.379(4)
C1–C6	1.521(4)
C2–C3	1.403(5)
C3–C4	1.357(6)
C4–C5	1.387(5)
Angles (deg)	
Cl1–Cu–Cl2	91.88(3)
Cl1–Cu–N1	97.23(7)
Cl1–Cu–N2	179.79(7)
Cl2–Cu–N1	170.89(7)
Cl2–Cu–N2	87.91(7)
N1–Cu–N2	82.98(9)
Cu–N1–C1	115.2(2)
Cu–N1–C5	126.4(2)
C1–N1–C5	118.4(3)
Cu–N2–C6	112.3(2)
N1–C1–C2	122.5(3)
N1–C1–C6	114.8(2)
C2–C1–C6	121.7(3)
C1–C2–C3	118.7(4)
C2–C3–C4	119.0(3)
C3–C4–C5	119.0(3)
N1–C5–C4	122.3(3)
N2–C6–C1	111.2(3)

TABLE VII. Fitted Parameters for Cu(L)Cl_2 using the Models described in Text. R represents the Normalized 'Goodness of Fit' Values.

	Cu(amp)Cl_2	Cu(aep)Cl_2
Curie-Weiss		
g	2.01	1.98
θ(K)	−5.9	−0.5
Dimer		
g	1.98	2.05
J/k	−8.0	−3.83
zJ'/k	−3.7	−0.12
R	101.4	1.00
Chain		
g	2.06	2.05
J/k	−7.11	−2.82
zJ'/k	−0.69	+0.1
R	1.00	30.8

fitting procedure using the values of the reduced magnetic susceptibility calculated by the authors. The quality of the fit was quite good to temperatures below the maximum in the magnetic susceptibility, but at the lowest temperatures ($T \cong 2.5$ K), an anomaly was observed in the magnetic data resulting in a departure from the linear chain model. The fit of the magnetic data to the Bonner-Fisher linear chain model is illustrated in Fig. 4 with the calculated curve drawn through the data points. To obtain the high quality of fitting illustrated in Fig. 4, a small molecular field correction (eqn. (3)) was required. The fitted parameters are listed in Table VII.

For the sake of completion, the linear chain model was also fitted to the magnetic data for $Cu(aep)Cl_2$. The quality of this fit was quite poor and the resulting parameters are included in Table VII.

Discussion

Our reanalysis of the magnetic data of $Cu(aep)Cl_2$ provides much the same conclusion as that obtained by Hodgson *et al.* [14, 25], however, we are now able to quantify the extent of interdimer interaction since we have incorporated the molecular field correction into the analysis. The quality of the theoretical fit of the dimer model (eqn. (2)) to the magnetic data increases dramatically when the model is corrected for the presence of interdimer exchange (eqn. (3)). We confirm that the magnetic properties of $Cu(aep)Cl_2$ are primarily dimeric but weak interdimer coupling is also present and the ratio zJ'/J is 0.03.

The magnetic analysis of $Cu(amp)Cl_2$ shows this complex to be primarily a one dimensional chain but with moderate interchain interactions. At the lowest temperature ($T < 2.5$ K) the magnetic susceptibility data deviate substantially from the theoretical linear chain values. This deviation, shown by a slight kink in the data is possibly the result of a magnetic phase transition with $T_c = 2.42$ K. To verify this hypothesis, high resolution low temperature magnetic susceptibility data and magnetic heat capacity data at temperatures in the vicinity of the observed anomaly need to be recorded on this complex.

It is also interesting to note that the bridging of $Cu(amp)Cl_2$, while at first glance of type 2 geometry, is actually quite intricate. The copper ions have two triply bridging chlorines attached to them. Each copper is coupled to its nearest neighbor and next nearest neighbor copper through one chlorine, while the other bridging chlorine couples the copper to its two nearest neighbors on each side. This 'ladder' type bridging geometry is illustrated schematically in Fig. 5. Other reported examples of ladder type linear chains include the $Cu(amp)Br_2$ analog [29]

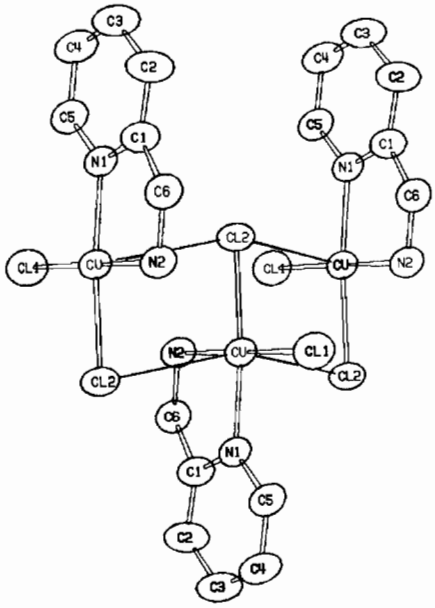

Fig. 5. Schematic diagram of the copper–chlorine bridging network for $Cu(amp)Cl_2$ linear chains.

as well as the chlorine bridged hydrazinium complex of copper(II) [31]. The zigzag propagation of the Cu(II) ions in the chain is uniform and there is little structural interaction between neighboring chains. The closest interchain copper–copper distance is 7.932(2) Å. Because of the bridging geometry, the copper(II) ions are effectively 6-coordinate in the linear chain structure. Any interchain magnetic exchange that is present is most likely to be propagated through a pyridine ring mediated superexchange pathway.

In light of the dimeric behavior of the analogous $Cu(aep)Cl_2$ complex, it is interesting to speculate about the cause of the low temperature kink in the magnetic susceptibility data of $Cu(amp)Cl_2$. The most likely explanation of the 2 K anomaly in the susceptibility data is a cooperative three dimensional antiferromagnetic phase transition (the moderate interchain coupling predicted by our theoretical analysis is consistent with this hypothesis). However, the dimeric forces present in the $Cu(aep)Cl_2$ complex may also affect $Cu(amp)Cl_2$. If this is true, a Spin Peierles transition could account for the anomalous low temperature magnetic susceptibility behavior. With the current data available, it would be foolhardy to make a definite assignment of this transition. Additional low temperature measurements on $Cu(amp)Cl_2$ are necessary before we can conclusively characterize the anomaly in the magnetic susceptibility data. We are currently making arrangements for these measurements.

Acknowledgement

C.J.O. would like to acknowledge the National Science Foundation Grant No. CHE 83-05707 for the purchase of the SQUID Susceptometer, and the CNRS of France and the UNO Research Council for support during the preparation of this manuscript.

References

1 R. D. Willett, D. Gatteschi and O. Kahn (eds.), 'Magneto Structural Correlations in Exchange Coupled Systems', in press.
2 C. J. O'Connor, *Prog. Inorg. Chem., 29*, 203 (1982).
3 O. Kahn, *Inorg. Chim. Acta, 62*, 3 (1982).
4 W. E. Hatfield, *Am. Chem. Soc. Symp. Ser., 5*, 2107 (1974); *Comments Inorg. Chem., 1*, 105 (1981).
5 D. J. Hodgson, *Am. Chem. Soc. Symp. Ser., 5*, 94 (1974).
6 D. J. Hodgson, *Prog. Inorg. Chem., 19*, 173 (1975).
7 V. H. Crawford, H. W. Richardson, J. R. Wasson, D. J. Hodgson and W. E. Hatfield, *Inorg. Chem., 15*, 2107 (1976).
8 B. Chiari, W. E. Hatfield, O. Piovesana, T. Tarantelli, L. W. Ter Harr and P. F. Zanozzi, *Inorg. Chem., 22*, 1468 (1983).
9 S. G. N. Roundhill, D. M. Roundhill, D. R. Bloomquist, C. Landee, R. D. Willett, D. M. Dooley and H. B. Gray, *Inorg. Chem., 18*, 831 (1979).
10 W. E. Marsh, K. C. Patel, W. E. Hatfield and D. J. Hodgson, *Inorg. Chem., 22*, 511 (1983).
11 J. A. Van Oijen and J. Reedijk, *Inorg. Chim. Acta, 25*, 131 (1977).
12 W. E. Hatfield, R. R. Weller and J. W. Hall, *Inorg. Chem., 19*, 3825 (1980).
13 P. D. W. Boyd, S. Mitra, C. L. Roston, G. L. Rowbottom and A. H. White, *J. Chem. Soc., Dalton Trans.*, 13 (1981).
14 V. C. Copeland, W. E. Hatfield and D. J. Hodgson, *Inorg. Chem., 12*, 1340 (1973).
15 P. W. Anderson, *Phys. Rev., 79*, 350 (1950).
16 Goodenough, *Phys. Rev., 100*, 564 (1955).
17 J. Kanamori, *J. Phys. Chem. Solids, 10*, 87 (1959).
18 A. P. Ginsberg, *Inorg. Chim. Acta Rev., 5*, 85 (1971).
19 P. J. Hay, J. C. Thibeault and J. Hoffmann, *J. Am. Chem. Soc., 97*, 4884 (1975).
20 M. F. Charlot, S. Jeannin, Y. Jeannin, O. Kahn, J. Lucrece-Abaul and J. Martin-Frere, *Inorg. Chem., 18*, 1675 (1979).
21 O. Kahn, J. Galy, Y. Journaux, J. Jaud and I. Morgenstern-Badarau, *J. Am. Chem. Soc., 104*, 2165 (1982).
22 O. Kahn and B. Briat, *J. Chem. Soc. Faraday Trans. 2, 72*, 268 (1976).
23 A. Bencini and D. Gatteschi, *Inorg. Chim. Acta, 31*, 11 (1978).
24 G. Von Kalkeren, W. W. Schmidt and R. Block, *Physica B & C, 97*, 315 (1979).
25 D. Y. Jeter, W. E. Hatfield and D. J. Hodgson, *J. Phys. Chem., 19*, 2707 (1972).
26 B. A. Frenz and Y. Okaya, 'Enraf-Nonius Structure Determination Package', Enraf-Nonius, Delft, Holland, 1982.
27 D. T. Cromer and J. T. Waber, 'International Tables for X-ray Crystallography, Vol. IV', Kynoch Press, Birmingham, 1974, Table 2.2B.
28 D. T. Cromer, 'International Tables for X-ray Crystallography, Vol. IV', Kynoch Press, Birmingham, 1974, Table 2.3.1.
29 H. M. Helis, H. Goodman, R. B. Wilson, J. A. Morgan and D. A. Hodgson, *Inorg. Chem., 16*, 2412 (1977).
30 J. C. Bonner and M. E. Fisher, *Phys. Rev. A:, 135*, 640 (1964).
31 D. B. Brown, J. A. Donner, J. W. Hall, S. R. Wilson, R. B. Wilson, D. J. Hodgson and W. E. Hatfield, *Inorg. Chem., 18*, 2635 (1979).